NON-UNIQUENESS OF T-CHARTS FOR SOLVING CC-ITL PROBLEMS WITH PASSIVE CHARACTERISTIC IMPEDANCES

K. Vudhivorn

Department of Electrical Engineering
Faculty of Engineering
Chulalongkorn University
Bangkok 10330, Thailand

D. Torrungrueng and C. Thimaporn

Department of Electrical and Electronic Engineering
Faculty of Engineering and Technology
Asian University
Chon Buri 20250, Thailand

Abstract—Conjugately characteristic-impedance transmission lines (CCITLs) implemented by lossless periodic transmission-line structures have found various applications in microwave technology, and the T-chart was developed to perform the analysis and design of CC-ITLs effectively. Originally, the normalization factor used in defining normalized impedances of the T-chart is the *geometric mean* of characteristic impedances of CCITLs, which is not only one possible choice. By using other normalization factors based on characteristic impedances, different graphical representations can be obtained; i.e., T-charts for CCITLs with passive characteristic impedances are *not unique*, and it depends on the associated normalization factor. In this study, *three* more possible normalization factors related to characteristic impedances of CCITLs are investigated. It is found that all T-charts for each normalization factor are strongly dependent on the argument of characteristic impedances of CCITLs in a complicated fashion. The original T-chart based on the geometric mean of characteristic impedances is found to be the most convenient graphical representation for solving CCITL problems.

Corresponding author: D. Torrungrueng (dtg@asianust.ac.th).

1. INTRODUCTION

Conjugately characteristic-impedance transmission lines (CCITLs) have found various applications in microwave technology [1–7]. Examples of CCITLs are reciprocal lossless uniform transmission lines (TLs), nonreciprocal lossless uniform TLs, exponentially tapered lossless nonuniform TLs [3, 8] and periodically loaded lossless TLs operated in passband [10–15]. In general, CCITLs are *lossless* and possess different characteristic impedances, which are *complex conjugate* of each other, for waves propagating in opposite directions. In the analysis and design of CCITLs, the analytical approach usually provides quite complicated formulas. In contrast, a graphical approach based on the T-chart provides a simpler way to obtain solutions with more physical insight [1–4].

Similar to the Smith chart for reciprocal uniform transmission lines, the T-chart is also the plot of normalized impedances and admittances in the reflection coefficient plane for CCITLs. For the Smith chart, the normalization factor used in defining normalized impedances is usually the characteristic impedance of reciprocal uniform transmission lines, which is always *unique*. For the original T-chart, the normalization factor is the *geometric mean* of characteristic impedances of CCITLs. However, it is not only one possible choice. Using other normalization factors based on characteristic impedances, different graphical representations can be obtained; i.e., T-charts for CCITLs are *not unique*, due to their dependence on normalization factors. In this study, *three* more possible normalization factors related to characteristic impedances of CCITLs are investigated. Only CCITLs with *passive* characteristic impedances are considered in this study.

This paper is organized as follows. Section 2 discusses the theory of CCITLs in brief. Section 3 presents how different T-charts can be obtained for each normalization factor. Graphical representations of different T-charts are depicted in Section 4. Finally, conclusions are provided in Section 5.

2. THEORY OF CCITLS

This section provides the necessary background on CCITLs for constructing all relevant T-charts in the next section. Figure 1 illustrates a CCITL terminated in a passive load impedance Z_L possessing the propagation constants, β^+ and β^-, with corresponding conjugate characteristic impedances, Z_0^+ and Z_0^- for propagation in the forward and reverse directions, respectively. Along the CCITL,
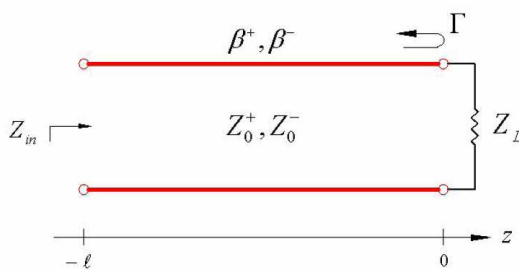
Figure 1. A CCITL terminated in a passive load impedance.

the travelling wave equations for phasor voltage $V(z)$ and the phasor current $I(z)$ can be written as [1]

$$V(z) = V_0^+ e^{-j\beta^+ z} + V_0^- e^{j\beta^- z} , \tag{1}$$

$$I(z) = \frac{V_0^+}{Z_0^+} e^{-j\beta^+ z} - \frac{V_0^-}{Z_0^-} e^{j\beta^- z} , \tag{2}$$

where $e^{-j\beta^+ z}$ and $e^{j\beta^- z}$ terms represent waves propagating in the $+z$ and $-z$ directions, respectively. By definition, the characteristic impedances of CCITLs $Z_0^{\pm}$ are complex conjugate of one another;

$$Z_0^+ = \left(Z_0^- \right)^* , \tag{3}$$

where the superscript "$*$" denotes the complex-conjugate symbol. For convenience, $Z_0^{\pm}$ are defined in a polar form as

$$Z_0^{\pm} = |Z_0| \, e^{\mp j\phi}, \tag{4}$$

where $|Z_0|$ and ϕ are the absolute value and argument of Z_0^-, respectively. For *passive* characteristic impedances ($\mathrm{Re}\{Z_0^{\pm} \geq 0\}$), (4) implies that the argument ϕ must lie in the following range:

$$-90° \leq \phi \leq 90°. \tag{5}$$

The voltage reflection coefficient at the load Γ is given by

$$\Gamma \equiv \frac{V_0^-}{V_0^+} = \frac{Z_L Z_0^- - Z_0^+ Z_0^-}{Z_L Z_0^+ + Z_0^+ Z_0^-}, \tag{6}$$

and the input impedance Z_{in} can be written compactly in terms of Γ as [1]

$$Z_{in} = Z_0^+ Z_0^- \frac{1 + \Gamma e^{-j\,2\tilde{\beta}\ell}}{Z_0^- - Z_0^+ \Gamma e^{-j\,2\tilde{\beta}\ell}} , \tag{7}$$

where the effective propagation constant $\tilde{\beta}$ is defined as

$$\tilde{\beta} \equiv \frac{1}{2}\left(\beta^+ + \beta^-\right). \tag{8}$$

For passive load terminations, the magnitude of the voltage reflection coefficient at the load is always less than or equal to unity [9]. In the next section, the construction of all alternative T-charts is illustrated.

3. CONSTRUCTION OF T-CHARTS

To construct all T-charts, the same concept as of constructing the Smith chart is employed. Similar to the Smith chart, T-charts are also the plot of normalized impedances and admittances in the voltage reflection coefficient plane for CCITLs. For the Smith chart, the normalization factor used in defining normalized impedances is usually the characteristic impedance of reciprocal uniform transmission lines, which is *unique*. For the original T-chart (also called a generalized ZY Smith chart) [1], the normalization factor $\tilde{Z}_0$ is the *geometric mean* of characteristic impedances of CCITLs; i.e., $\tilde{Z}_0 = \sqrt{Z_0^+ Z_0^-} = |Z_0|$, which is always real. However, it is not only one possible choice. In this study, *three* more possible normalization factors related to characteristic impedances of CCITLs are investigated; i.e., the arithmetic mean of Z_0^+ and Z_0^- (Case 1), Z_0^- (Case 2) and Z_0^+ (Case 3). Only passive load terminations are of interest in this study; i.e., the region of interest is within or on the unit circle in the Γ plane.

For Case 1, the normalization factor $\tilde{Z}_0$ is

$$\tilde{Z}_0 = \frac{Z_0^+ + Z_0^-}{2} = |Z_0 \cos \phi| = |Z_0| \cos \phi, \tag{9}$$

where $\cos \phi \geq 0$ for passive characteristic impedances (see (5)). Note that $\tilde{Z}_0$ is real in this case. The normalized impedance z of an arbitrary impedance Z is defined as

$$z \equiv \frac{Z}{\tilde{Z}_0}. \tag{10}$$

Using (6), (9) and (10), the normalized load impedance z_L can be written compactly in terms of Γ as

$$z_L = \frac{1 + \Gamma}{\cos \phi \left(e^{j\phi} - \Gamma e^{-j\phi}\right)}, \tag{11}$$

where $\Gamma \equiv \Gamma_r + j\Gamma_i$ and $z_L \equiv r_L + jx_L$. After rearranging the real and imaginary parts of (11), the resistance and reactance circles can

be obtained respectively as follows:

$$\left(\Gamma_r - \frac{r_L \cos 2\phi}{r_L + 1}\right)^2 + \left(\Gamma_i - \frac{r_L \sin 2\phi}{r_L + 1}\right)^2 = \left(\frac{1}{r_L + 1}\right)^2, \quad (12)$$

$$\left[\Gamma_r - \left(\frac{x_L \cos 2\phi - \tan \phi}{x_L + \tan \phi}\right)\right]^2 + \left[\Gamma_i - \left(\frac{x_L \sin 2\phi + 1}{x_L + \tan \phi}\right)\right]^2 = \left(\frac{1}{x_L + \tan \phi}\right)^2. \quad (13)$$

Using the same procedure as above, equations of the conductance and susceptance circles of Case 1 can be obtained respectively as follows:

$$\left[\Gamma_r + \left(\frac{g_L}{g_L + \cos^2 \phi}\right)\right]^2 + \Gamma_i^2 = \left(\frac{\cos^2 \phi}{g_L + \cos^2 \phi}\right)^2, \quad (14)$$

$$(\Gamma_r + 1)^2 + \left[\Gamma_i + \left(\frac{\cos^2 \phi}{b_L - \sin \phi \, \cos \phi}\right)\right]^2 = \left(\frac{\cos^2 \phi}{b_L - \sin \phi \, \cos \phi}\right)^2, \quad (15)$$

where g_L and b_L are the real and imaginary parts of the normalized load admittance $y_L = 1/z_L$.

For Case 2, the normalization factor is

$$\widetilde{Z}_0 = Z_0^- = |Z_0| \, e^{j\phi}, \quad (16)$$

which is complex in general. Following the same procedure as in Case 1, these four circle equations can be obtained as follows:

$$\left[\Gamma_r - \left(\frac{2r_L \cos 2\phi - 1 + \cos 2\phi}{2(r_L + 1)}\right)\right]^2 + \left[\Gamma_i - \left(\frac{2r_L \sin 2\phi + \sin 2\phi}{2(r_L + 1)}\right)\right]^2$$
$$= \left[\frac{\sqrt{2} \cos 2\phi + 2}{2(r_L + 1)}\right]^2, \quad (17)$$

$$\left[\Gamma_r - \left(\frac{2x_L \cos 2\phi - \sin 2\phi}{2x_L}\right)\right]^2 + \left[\Gamma_i - \left(\frac{2x_L \sin 2\phi + \cos 2\phi + 1}{2x_L}\right)\right]^2$$
$$= \left[\frac{\sqrt{2} \cos 2\phi + 2}{2x_L}\right]^2, \quad (18)$$

$$\left[\Gamma_r + \left(\frac{2g_L - \cos 2\phi + 1}{2(g_L + 1)}\right)\right]^2 + \left[\Gamma_i - \left(\frac{\sin 2\phi}{2(g_L + 1)}\right)\right]^2 = \left[\frac{\sqrt{2} \cos 2\phi + 2}{2(g_L + 1)}\right]^2, \quad (19)$$

$$\left[\Gamma_r + \left(\frac{2b_L - \sin 2\phi}{2b_L}\right)\right]^2 + \left[\Gamma_i + \left(\frac{\cos 2\phi + 1}{2b_L}\right)\right]^2 = \left[\frac{\sqrt{2} \cos 2\phi + 2}{2b_L}\right]^2, \quad (20)$$

for resistance, reactance, conductance and susceptance circles, respectively.

For Case 3, the normalization factor is

$$\widetilde{Z}_0 = Z_0^+ = |Z_0| \, e^{-j\phi}, \quad (21)$$

which is complex in general. Following the same procedure as in Case 1, these four circle equations for resistance, reactance, conductance and susceptance are given as follows:

$$\left[\Gamma_r - \left(\frac{2r_L\cos 2\phi - \cos 2\phi + 1}{2\left(r_L + \cos 2\phi\right)}\right)\right]^2 + \left[\Gamma_i - \left(\frac{2r_L\sin 2\phi - \sin 2\phi}{2\left(r_L + \cos 2\phi\right)}\right)\right]^2$$
$$= \left[\frac{\sqrt{2\cos 2\phi + 2}}{2\left(r_L + \cos 2\phi\right)}\right]^2, \tag{22}$$

$$\left[\Gamma_r - \left(\frac{2x_L\cos 2\phi - \sin 2\phi}{2\left(x_L + \sin 2\phi\right)}\right)\right]^2 + \left[\Gamma_i - \left(\frac{2x_L\sin 2\phi + \cos 2\phi + 1}{2\left(x_L + \sin 2\phi\right)}\right)\right]^2$$
$$= \left[\frac{\sqrt{2\cos 2\phi + 2}}{2\left(x_L + \sin 2\phi\right)}\right]^2, \tag{23}$$

$$\left[\Gamma_r + \left(\frac{2g_L + \cos 2\phi - 1}{2\left(g_L + \cos 2\phi\right)}\right)\right]^2 + \left[\Gamma_i + \left(\frac{\sin 2\phi}{2\left(g_L + \cos 2\phi\right)}\right)\right]^2$$
$$= \left[\frac{\sqrt{2\cos 2\phi + 2}}{2\left(g_L + \cos 2\phi\right)}\right]^2, \tag{24}$$

$$\left[\Gamma_r + \left(\frac{2b_L - \sin 2\phi}{2\left(b_L - \sin 2\phi\right)}\right)\right]^2 + \left[\Gamma_i + \left(\frac{\cos 2\phi + 1}{2\left(b_L - \sin 2\phi\right)}\right)\right]^2 = \left[\frac{\sqrt{2\cos 2\phi + 2}}{2\left(b_L - \sin 2\phi\right)}\right]^2, \tag{25}$$
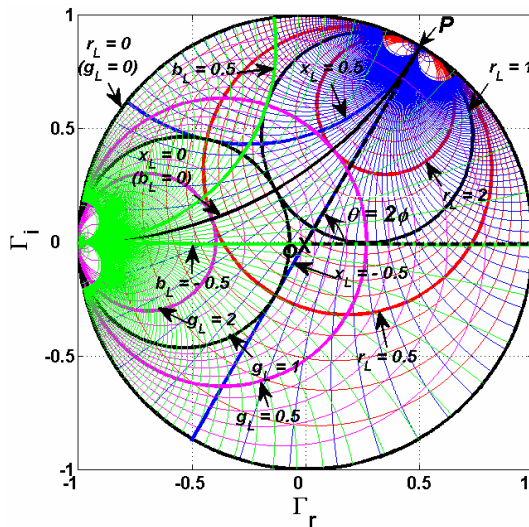
respectively.

Figure 2. The original ZY T-chart using $\tilde{Z}_0 = |Z_0|$ with $\phi = 30°$.

Note that the normalization factors for these three cases depend on both $|Z_0|$ and ϕ, while the original normalization factor based on the geometric mean of $Z_0^{\pm}$ depends only on $|Z_0|$. In addition, it is found that those four circle equations of these cases are reduced to be identical to those of the standard Smith chart when $\phi = 0°$ as expected. Next, examples of graphical representations of T-charts for each case are depicted in Section 4.

4. GRAPHICAL REPRESENTATIONS OF EACH T-CHART

In Section 3, it is found that all T-charts strongly depend on the argument ϕ in a complex fashion. To illustrate these dependences, consider T-charts for each case, including the original T-chart [1], when $\phi = 30°$ and $\phi = -30°$. Figure 2 illustrates the plot of the original ZY T-chart using $\tilde{Z}_0 = \sqrt{Z_0^+ Z_0^-} = |Z_0|$ with $\phi = 30°$. In addition, Figures 3 to 5 illustrate the plot of the ZY T-charts of Cases 1, 2 and 3 in the Γ plane with $\phi = 30°$, respectively. The horizontal line and the line $\overline{OP}$, drawn from the origin O in the Γ plane to the *touching point* P of all reactance circles, intersect each other at the angle θ. Note that the point P in Figures 2 to 5 is the same point. In addition, it is
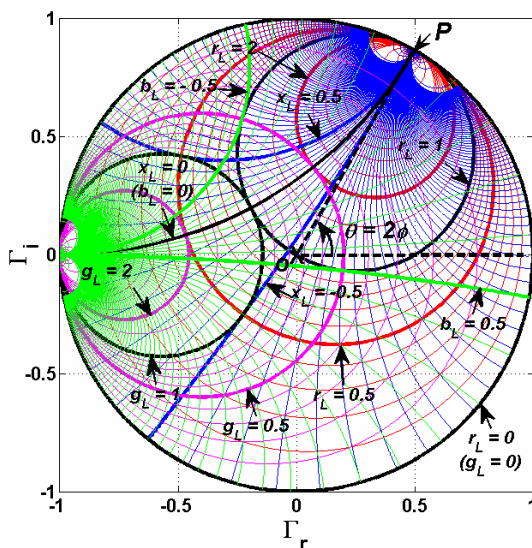
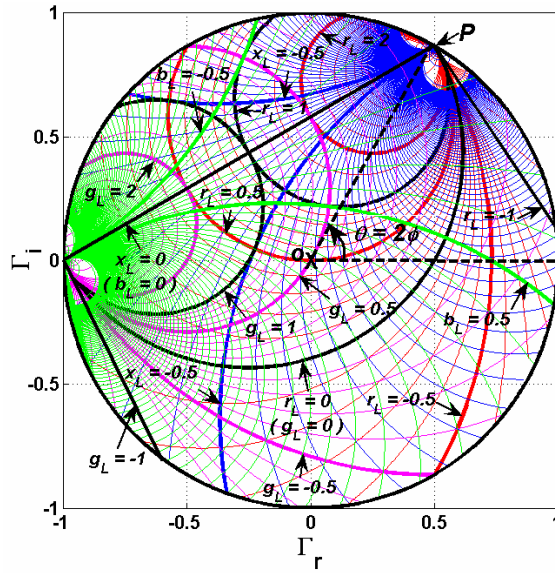

Figure 3. The ZY T-chart of Case 1 with $\phi = 30°$.

Figure 4. The ZY T-chart of Case 2 with $\phi = 30°$.

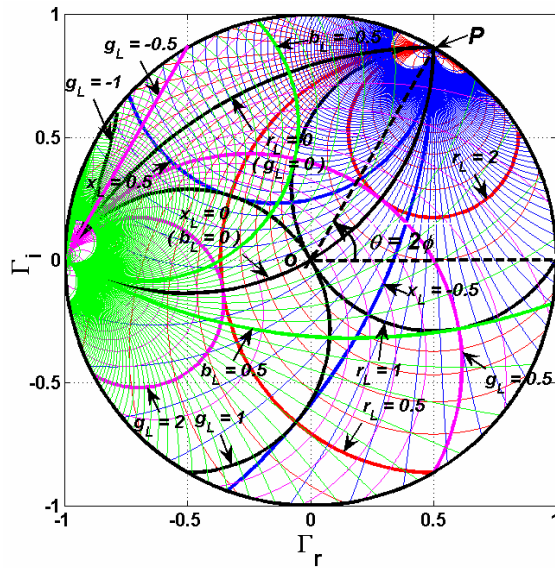**Figure 5.** The ZY T-chart of Case 3 with $\phi = 30°$.

found that the relationship between the argument ϕ and the angle θ is given by

$$\theta = 2\phi. \tag{26}$$

In this case, θ is equal to $60°$ for $\phi = 30°$. Note that impedance and admittance scales for each T-chart are different.

Figure 6 illustrates the plot of the original ZY T-chart using $\tilde{Z}_0 = |Z_0|$ with $\phi = -30°$. In addition, Figures 7 to 9 illustrate the plots of the ZY T-charts in the Γ plane with $\phi = -30°$ for Cases 1, 2 and 3, respectively. Using (26) with $\phi = -30°$, θ is equal to $-60°$ in this case. Note that impedance and admittance scales for each T-chart are different as well.

From Figures 2 to 9, it is observed that the circle $r_L = 0$ $(g_L = 0)$ is always the unit circle for $\tilde{Z}_0 = |Z_0|$ (geometric mean) and $\tilde{Z}_0 = |Z_0| \cos \phi$ (arithmetic mean) as shown in Figures 2, 3, 6 and 7, and all circles $r_L > 0$ and all circles $g_L > 0$ are always within the unit circle. For the normalization factors of Cases 2 and 3, the circle $r_L = 0$ $(g_L = 0)$ is not the unit circle in general as shown in Figures 4, 5, 8 and 9, and the circles $r_L < 0$ and the circles $g_L < 0$ can exist within the unit circle.

Comparing $\tilde{Z}_0 = |Z_0|$ (geometric mean) and $\tilde{Z}_0 = |Z_0| \cos \phi$ (arithmetic mean), it can be noticed that both normalization factors
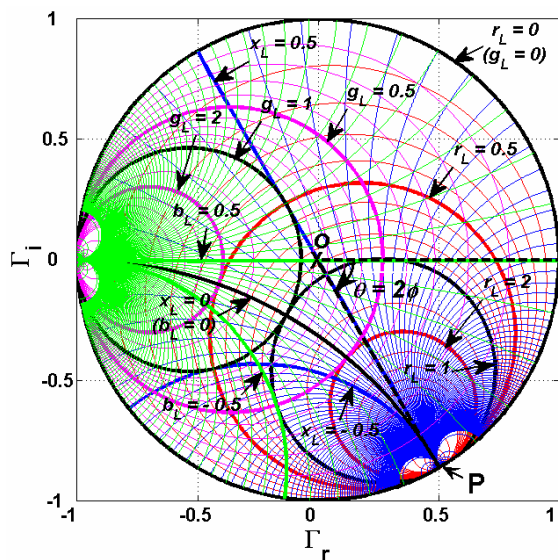
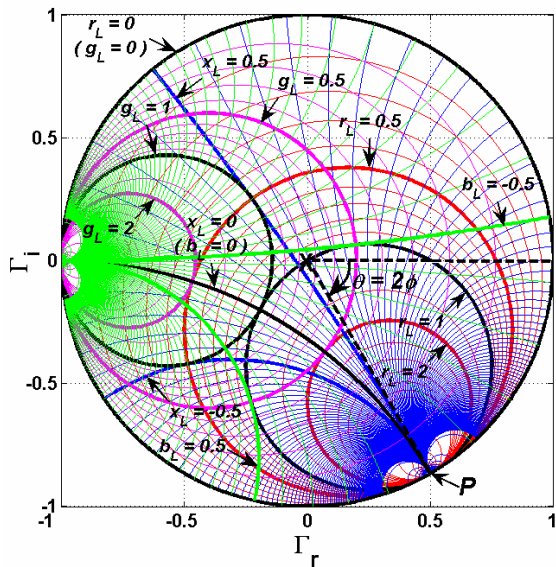**Figure 6.** The original ZY T-chart using $\tilde{Z}_0 = |Z_0|$ with $\phi = -30°$.

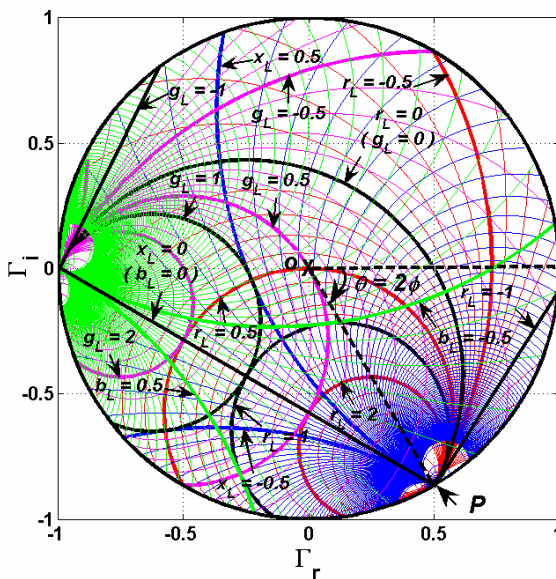**Figure 7.** The ZY T-chart of Case 1 with $\phi = -30°$.

Figure 8. The ZY T-chart of Case 2 with $\phi = -30°$.

are always real. In addition, $\tilde{Z}_0 = |Z_0|$ does not depend on ϕ unlike $\tilde{Z}_0 = |Z_0|\cos\phi$. It can also be observed that when $\phi \to \pm\frac{\pi}{2}$, the normalized impedance $(z = Z/\tilde{Z}_0)$ of $\tilde{Z}_0 = |Z_0|\cos\phi$ approaches infinity, which is not convenient in usage. On the other hand, both normalization factors of Cases 2 and 3 are *complex* in general and depend on ϕ. Therefore, the normalized impedances of Cases 2 and 3 change their physical meanings of the original unnormalized impedances. For example, when the load impedance is real, the normalized impedances of Cases 2 and 3 generally become complex numbers due to the normalization process, which may cause misleading to users. As a result, some passive load impedances may possibly yield a negative normalized resistance when using the normalization factors of Cases 2 or 3 as shown in Figures 4, 5, 8, and 9. Based on the above observations, the original normalization factor of $\tilde{Z}_0 = |Z_0|$ (geometric mean) is the best for solving CCITL problems because it is real and independent of ϕ.
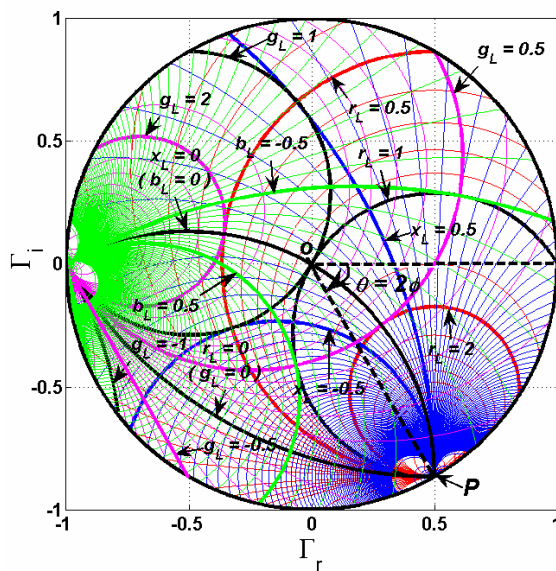

Figure 9. The ZY T-chart of Case 3 with $\phi = -30°$.

5. CONCLUSION

It is found that all four considered T-charts for each normalization factor are strongly dependent on the argument ϕ of characteristic impedances of CCITLs in a complicated fashion. In addition, these T-charts are reduced to the Smith chart when $\phi = 0°$ as expected. Procedures of using all T-charts for solving CCITL problems are similar to those of using the Smith chart. In a preliminary study, it is found that all T-charts yield the same input impedances for given terminated CCITLs as expected. Among these T-charts, the original T-chart with the normalization factor of the *geometric mean* of Z_0^+ and Z_0^- is the most convenient chart for solving CCITL problems with passive characteristic impedances as pointed out earlier at the end of Section 4.

REFERENCES

1. Torrungrueng, D. and C. Thimaporn, "A generalized ZY Smith chart for solving nonreciprocal uniform transmission-lines problems," *Microwave and Optical Technology Letters*, Vol. 40, No. 1, 57–61, 2004.
2. Torrungrueng, D. and C. Thimaporn, "Applications of the ZY T-chart for nonreciprocal stub tuner," *Microwave and Optical Technology Letters*, Vol. 45, No. 3, 259–262, 2005.
3. Torrungrueng, D. and C. Thimaporn, "Applications of the T-chart for solving exponentially tapered lossless nonuniform transmission-lines problems," *Microwave and Optical Technology Letters*, Vol. 45, No. 3, 402–406, 2005.
4. Torrungrueng, D., C. Thimaporn, and N. Chamnandechakun, "An applications of the T-chart for solving problems associated with terminated finite lossless periodic structures," *Microwave and Optical Technology Letters*, Vol. 47, No. 6, 594–597, 2005.
5. Lamultree, S. and D. Torrungrueng, "On the characteristics of conjugately characteristic impedance transmission lines with active characteristic impedance," *Proceedings of the 2006 Asia-Pacific Microwave Conference*, Vol. 1, 225–228, Yokohama, Japan, December 2006.
6. Torrungrueng, D., P. Y. Chou, and M. Krairiksh, "An extended ZY T-chart for conjugately characteristic impedance transmission lines with active characteristic impedances," *Microwave and Optical Technology Letters*, Vol. 49, No. 8, 1961–1964, 2007.
7. Torrungrueng, D. and S. Lamultree, "Equivalent graphical solutions of terminated conjugately characteristic-impedance

transmission lines with non-negative and corresponding negative characteristic resistance," *Progress In Electromagnetics Research*, PIER 92, 137–151, 2009.

8. Wu, Y. and Y. Liu, "Standard Smith chart approach to solve exponential tapered nonuniform transmission line problems," *Journal of Electromagnetic Waves and Applications*, Vol. 22, No. 11–12, 1639–1646, 2008.

9. Torrungrueng, D., S. Lamultree, C. Phongcharoenpanich, and M. Krairiksh, "In-depth analysis of reciprocal periodic structures of transmission lines," *IET Microwaves, Antennas and Propagation*, Vol. 3, 591–600, 2009.

10. Zhu, Y. and R. Lee, "Tvfem analysis of periodic structures for radiation and scattering," *Progress In Electromagnetic Research*, PIER 25, 1–22, 2000.

11. Khalaj-Amirhosseini, M., "Analysis of periodic and aperiodic coupled nonuniform transmission lines using the fourier series expansion," *Progress In Electromagnetics Research*, PIER 65, 15–26, 2006.

12. Lu, W. and T.-J. Cui, "Efficient method for full-wave analysis of large-scale finite-sized periodic structures," *Journal of Electromagnetic Waves and Application*, Vol. 21, No. 14, 2157–2168, 2007.

13. Du, P., B.-Z. Wang, H. Li, and G. Zheng, "Scattering analysis of large-scale periodic structures using the sub-entire domain basis function method and characteristic function method," *Journal of Electromagnetic Waves and Application*, Vol. 21, No. 14, 2085–2094, 2007.

14. Fardis, M. and R. Khosravi, "Analysis of periodically loaded suspended substrate structures in millimeter wave," *Progress In Electromagnetics Research B*, Vol. 3, 143–156, 2008.

15. Lu, W. B., Q. Y. Zhao, and T.-J. Cui, "Sub-entire-domain basis function method for irrectangular periodic structures," *Progress In Electromagnetics Research B*, Vol. 5, 91–105, 2008.